CCFE
CULHAM CENTRE FOR FUSION ENERGY

UK Atomic Energy Authority

UKAEA-CCFE-PR(22)09

P.A. Schneider, C. Angioni, L. Frassinetti, L. Horvath, M. Maslov, F. Auriemma, M. Cavedon, C.D. Challis, E. Delabie, M.G. Dunne, J.M. Fontdecaba Climent, J. Hobirk, A. Kappatou, D.L. Keeling, B. Kurzan, M. Lennholm, B. Lomanovski, C.F. Maggi, R.M. McDermott, T. Pütterich, A. Thorman, M. Willensdorfer

THE DEPENDENCE OF CONFINEMENT ON THE ISOTOPE MASS IN THE CORE AND THE EDGE OF AUG AND JET-ILW H-MODE PLASMAS

THE DEPENDENCE OF CONFINEMENT ON THE ISOTOPE MASS IN THE CORE AND THE EDGE OF AUG AND JET-ILW H-MODE PLASMAS

P.A. Schneider, C. Angioni, L. Frassinetti, L. Horvath, M. Maslov, F. Auriemma, M. Cavedon, C.D. Challis, E. Delabie, M.G. Dunne, J.M. Fontdecaba Climent, J. Hobirk, A. Kappatou, D.L. Keeling, B. Kurzan, M. Lennholm, B. Lomanovski, C.F. Maggi, R.M. McDermott, T. Pütterich, A. Thorman, M. Willensdorfer

This is a preprint of a paper submitted for publication in Nuclear Fusion

THE DEPENDENCE OF CONFINEMENT ON THE ISOTOPE MASS IN THE CORE AND THE EDGE OF AUG AND JET-ILW H-MODE PLASMAS

P. A. Schneider[1], C. Angioni[1], L. Frassinetti[2], L. Horvath[3], M. Maslov[3], F. Auriemma[4], M. Cavedon[1], C. D. Challis[3], E. Delabie[5], M. G. Dunne[1], J. M. Fontdecaba Climent[3], J. Hobirk[1], A. Kappatou[1], D. L. Keeling[3], B. Kurzan[1], M. Lennholm[3], B. Lomanovski[3], C. F. Maggi[3], R. M. McDermott[1], T. Pütterich[1], A. Thorman[3], M. Willensdorfer[1], the ASDEX Upgrade Team[a], the EUROfusion MST1 Team[b] and JET Contributors[c]

[1]Max-Planck-Institut für Plasmaphysik, Boltzmannstr. 2, 85748 Garching, Germany
[2]KTH Royal Institute of Technology, Teknikringen 31, Sweden
[3]United Kingdom Atomic Energy Authority, Culham Centre for Fusion Energy, Culham Science Centre, Abingdon, Oxon, OX14 3DB, UK
[4]Consorzio RFX-CNR, ENEA, INFN, Università di Padova, Acciaierie Venete SpA, Padova, Italy, CNR-ISTP, Corso Stati Uniti 4, 35127 Padova, Italy
[5]Oak Ridge National Laboratory, Oak Ridge, Tennessee, United States of America
[a]See author list of H. Meyer et al. 2019 Nucl. Fusion 59 112014
[b]See author list of B. Labit et al. 2019 Nucl. Fusion 59 086020
[c]See the author list of 'Overview of JET results for optimising ITER operation' by J. Mailloux et al to be published in Nuclear Fusion Special issue: Overview and Summary Papers from the 28th Fusion Energy Conference (Nice, France, 10-15 May 2021)

Abstract

Experiments in ASDEX Upgrade (AUG) and JET with the ITER-like wall (JET-ILW) are performed to separate the pedestal and core contributions to confinement in H-modes with different main ion masses. A strong isotope mass dependence in the pedestal is found which is enhanced at high gas puffing. This is because the ELM type changes when going from D to H for matched engineering parameters, which is likely due to differences in the inter ELM transport with isotope mass. With different triangularity the pedestal can be matched between H and D while keeping the engineering parameters relevant for core transport the same. With matched pedestals Astra /TGLF (Sat1geo) core transport simulations predict the experimental profiles equally well for H and D. The simulations for matched parameters show only a small negative mass dependence and no gyro-Bohm scaling is observed. However, to match the experimental observations at medium β it is required to take the fast-ion dilution and rotation into account. This is not enough for high β plasmas where for the first time a profile match between H and D plasmas was achieved experimentally. Under these conditions quasilinear modelling with TGLF over predicts the transport in the core of H and D plasmas alike.

1 Introduction

The isotope mass dependence of confinement is a long standing open question in tokamak physics. In multi-machine studies the global confinement time is found to scale with $M^{0.2}$ where M is the main ion mass number [1]. However, this global number incorporates edge and core physics at the same time while we know that they can scale differently [2]. To address this question a series of discharges has been conducted with highly resolved measurements to identify the various contributions to the isotope mass dependence of confinement in the tokamaks ASDEX Upgrade (AUG) and JET with the ITER-like wall (JET-ILW).

AUG and JET-ILW are both metal tokamaks with a tungsten divertor. In AUG also the main chamber walls are tungsten while in JET-ILW they are coated with beryllium, which

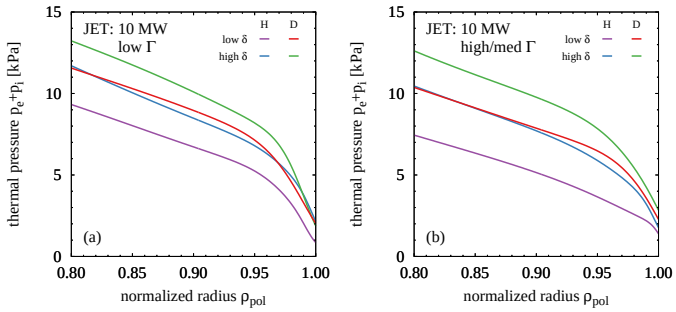

FIG. 1: Total pressure at the edge for H and D plasmas with different shaping and different gas puffing. Low gas puffing $\Gamma \sim 0.9 \cdot 10^{22}/s$ *(a) (H: JPN97095, D: JPN97036) and medium (D: JPN97035) to high (H: JPN97094) gas puffing* $\Gamma \sim 13 - 18 \cdot 10^{22}/s$

is the setup foreseen for ITER. The metal wall results in a relatively low concentration of low Z impurities and consequently an effective charge Z_{eff} of typically below 1.5 in both devices. To improve ion temperature measurements small amounts of low-Z impurities are introduced into the plasma externally. In JET-ILW this is neon in H and D plasmas and in AUG nitrogen in H plasmas. The main plasma parameters in AUG are a plasma current of $I_{\text{p}} = 0.8$ MA and a toroidal magnetic field $B_{\text{t}} = -2.5$ T with an edge safety factor of $q_{95} = 5.2$. In JET-ILW $I_{\text{p}} = 1.4$ MA and $B_{\text{t}} = 1.7$ T with $q_{95} = 3.7$ is used with the C/C divertor configuration which has the strike points in the inner and outer corner a configuration similar to the closed divertor of AUG. The applied heating power is between 7-22 MW in AUG and 5-15 MW in JET-ILW. Since JET-ILW is twice the size of AUG, JET-ILW has about 2/3 lower $\rho_\star$ than AUG. The difference in size also means the power density in AUG is substantially higher than in JET-ILW for the presented discharge set, which results in higher relative fast-ion content in AUG compared to JET-ILW.

In order to overcome the limitation of the NBI in hydrogen and to achieve higher NBI heating powers, D-NBI heating is used for dominantly H and D plasmas. This decreases the isotope purity of the plasma and H concentrations of $n_{\text{H}}/(n_{\text{H}} + n_{\text{D}}) \simeq 0.9$ are achieved. While not discussed in detail here, no indication was found that the residual 10% of D alters the main conclusions of this study. D plasmas in JET-ILW have 1-2% residual H while it is up to 5% in AUG. The gas puffing rate Γ will be quoted as 'low' or 'high'. A low Γ is in both machines close to the lowest puffing rate for which the plasmas are considered reliably stable against impurity accumulation. A high Γ is a multiple of the low gas puffing rate.

Along with the main ion mass, the heating power P, gas puffing and plasma triangularity δ are varied in AUG and JET-ILW. In JET-ILW the strike points are kept constant for the different δ which is crucial to avoid the impact of varying divertor configurations. First we will describe the impact on the pedestal in section 2, then we select pairs with matched pedestal for a detailed core transport analysis in section 3 and discuss the core-edge coupling for the whole data set.

2 Edge pedestal

The pedestal shows a strong dependence on the main ion mass in AUG [3–5] as well as in JET-ILW [6,7], most notably the pedestal density is lower in H for matched engineering parameters - like power, gas, plasma shape - while the temperatures can be similar resulting in lower pressure. To understand the origin of this difference we are discussing the three main factors which set the pedestal top: ELM stability, ELM losses and inter ELM transport.

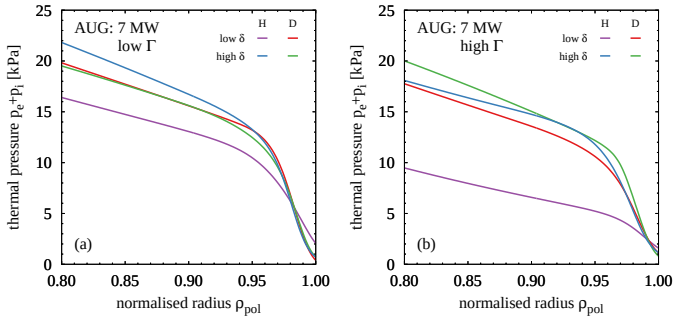

FIG. 2: Total pressure at the edge for H and D plasmas with different shaping and different gas puffing. Low gas puffing $\Gamma \sim 0.1 \cdot 10^{22}/s$ *(a) (H: AUG35230, D: AUG35852) and high (H: AUG34716, AUG35231, D: AUG35852) gas puffing* $\Gamma \sim 7 - 8 \cdot 10^{22}/s$

ELM stability is the main candidate. In principle, a mass dependence could be introduced via diamagnetic stabilisation [8], however, this effect was found to be small for the JET-ILW pulses discussed here [7]. Profile parameters which change between H and D can have an impact on the ELM stability. A shift of the density profile or an increasing separatrix density lowers the pedestal pressure at which ELMs are triggered [9, 10]. Also an increase of the separatrix temperature due to changes in the divertor condition can have an influence on the ELM stability [7]. Both mechanisms are included in the following analysis.

ELM losses $P_{\mathrm{loss,ELM}}$ were found to have an impact on the pedestal top in D plasmas [11]. Since the ELM behaviour is different in H and D plasmas, with typically higher frequencies in H, this was tested in AUG [3] and JET-ILW [7]. However, since the ELM frequency is strongly correlated to the ELM size, $P_{\mathrm{loss,ELM}}$ is not varying enough between isotopes to be sufficient to explain the observed differences in the pedestal. This is why we assume the impact of the ELM losses to be negligible.

The inter ELM transport, is the least understood part of the three candidates to explain the isotope dependence in the pedestal. The theoretical understanding of the heat and particle transport in the H-mode pedestal is an active field of research, however, due to the steep gradients reliable simulations are difficult, but can be expected in the upcoming years. For L-mode plasmas drift waves were found in the edge and show properties explaining the observed mass dependence of transport [12,13] and it is possible that collisional drift waves also play an important role in H-mode. While interpretative experimental studies regularly find that the transport in H is larger than in D [7,14], the uncertainties in these studies are substantial. In particular, due to the mass dependence in the pedestal a trade off between matching the sources or matching the profiles has to be made. Due to the lack of theoretical understanding of the pedestal physics it is difficult to distinguish a source related impact (profile stiffness, electron-ion equipartition) or changing profiles (collisionality, $T_\mathrm{i}/T_\mathrm{e}$, etc.) from the actual impact the ion mass has. Because of these difficulties we developed a new strategy for isotope studies which allows us to keep the sources the same while also matching the profiles of H and D plasma. This is done by changing the plasma triangularity δ. Although, we have to understand the impact of δ now, this opens up an angle for investigation of the isotope mass dependence complementary to previous studies relying on source or profile changes.

In figure 1 the total plasma pressure is plotted at the plasma edge for different triangularity δ and gas puffing Γ in JET-ILW. For low gas puffing (a) as well as medium to high gas puffing (b) one observes a clear correlation of the pedestal top pressure and isotope mass, namely lower pressure in H compared to D. When comparing low δ D with high δ H plasmas, however, we find an exceptional agreement of the pressure at the pedestal top

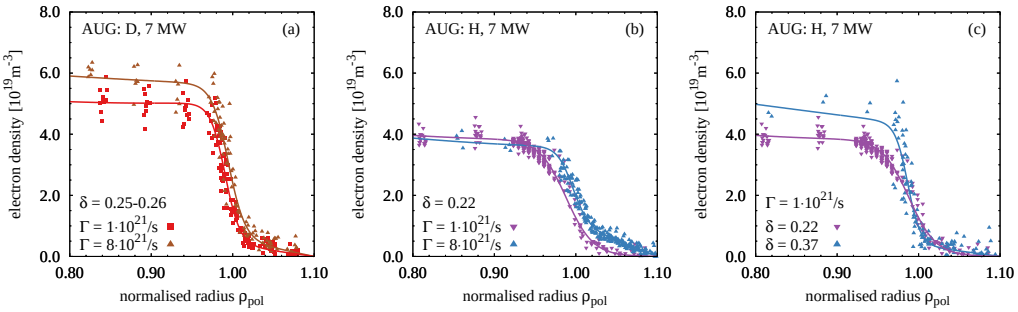

FIG. 3: Electron density profiles for different gas puffing in D (AUG35852) (a) and in H (AUG34716, AUG35230) (b) as well as different δ at low gas puffing in H (AUG35230) (c). [5]

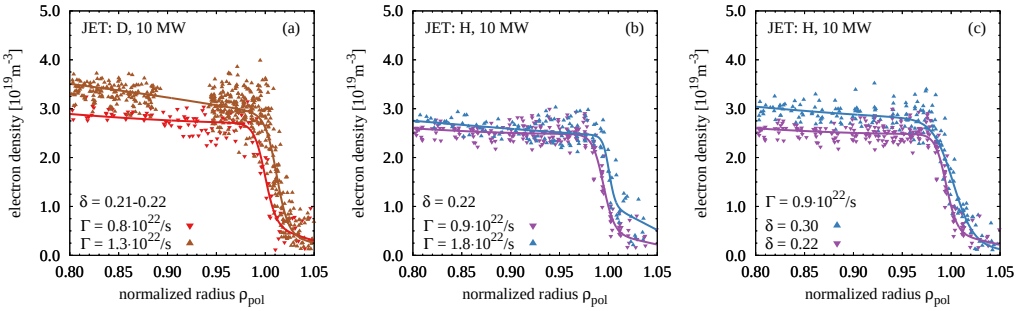

FIG. 4: Electron density profiles for different gas puffing in D (JPN87344, JPN97036) (a) and in H (JPN97094, JPN97095) (b) as well as different δ at low gas puffing in H (JPN97095) (c).

for constant input power. This is observed for low (a) and high (b) Γ as shown in figure 1 for JET-ILW and in figure 2 for AUG. In both machines the higher δ offsets the reduction in pressure as introduced by the main ion mass. This is true at low and high Γ which show a different pressure reduction at low δ. This is an indication that the impact of the triangularity is non-linear, which could include a phase transition.

With the variation in the triangularity for the first time a matched pedestal could be obtained in plasmas with different main ion mass while keeping the heating and gas fuelling the same. A matched pedestal is also beneficial for the core transport analysis discussed in section 3.

The density pedestal is key in understanding the differences in pressure. The phenomenology of the density pedestal is remarkably similar in AUG and JET-ILW. This is evident when comparing the profiles shown in figure 3 and figure 4. In (a) the density increases with increasing gas puff Γ in the D plasmas due to increasing density at the separatrix. This is expected when the ELM behaviour does not change significantly. The same increase in Γ applied to an H plasma does not increase the pedestal top density shown in (b). Simultaneously the total pedestal pressure is reduced by 40% (JET-ILW) and 70% (AUG), as was shown in figure 1 and figure 2, which for constant density has to be due to a lower temperature. However, when changing δ the density can be increased in H as shown in (c) and match the D pedestal density at the same gas fuelling without degrading the pedestal temperature. In AUG changing δ and Γ had a strong impact on the inter ELM density fluctuation amplitude, measured in the pedestal region with Doppler reflectometry, with high δ showing lower fluctuation levels [5]. While being no proof this is a strong indication that the particle transport changes with δ and Γ.

As discussed above, the most obvious candidate to understand the pedestal is the ELM stability. The review of the density profiles indicates that the shifted position of the density profile might indeed contribute to the lower pedestal pressure in H. To test this hypothesis

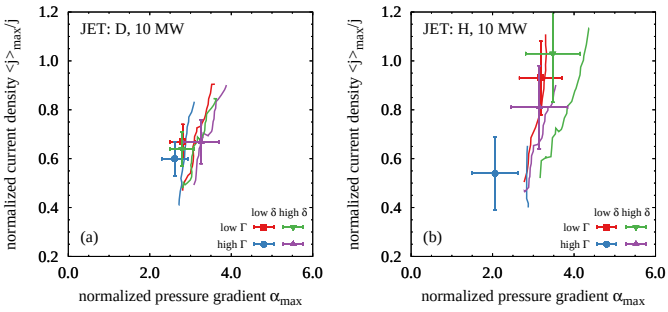

FIG. 5: Diagrams of the normalized edge current density $\langle j \rangle_{\max}/j$ and normalized pressure gradient $\alpha_{\max}$ with the peeling-ballooning stability boundary and the operational point from experiment for a triangularity δ and gas puff Γ scan with main ion mass D (a) and H (b) in JET-ILW.

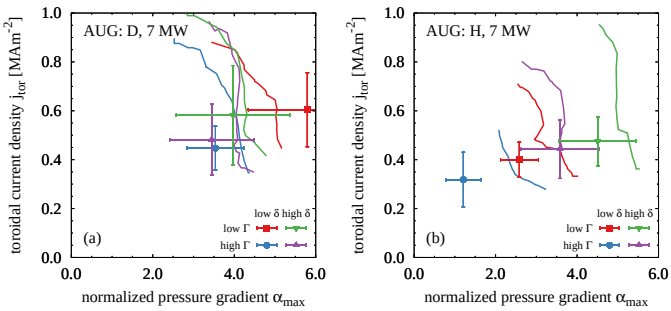

FIG. 6: Diagrams of the toroidal current density j_{tor} and normalized pressure gradient $\alpha_{\max}$ with the peeling-ballooning stability boundary and the operational point from experiment for a triangularity δ and gas puff Γ scan with main ion mass D (a) and H (b) in AUG. [5]

the pedestal stability against peeling-ballooning modes is studied using ELITE (JET-ILW) and MISHKA (AUG) with a HELENA equilibrium, the results are shown in figure 5 for the JET-ILW plasmas and figure 6 for the AUG plasmas.

The stability boundary where the growth rate $\gamma = 0.03$ is indicated as a line. For values of $\langle j \rangle_{\max}/j$, $\alpha_{\max}$ lower than the boundary the pedestal is considered stable against peeling-ballooning modes. For D we find the stability boundaries for all cases fairly close to each other with the high δ cases tending towards higher $\alpha_{\max}$ as expected. The stability boundaries for the JET-ILW plasmas shown in figure 5 are found around $\alpha_{\max} \sim 3$ for H and D alike. This suggests that from ideal peeling-ballooning modes no contribution to the observed difference with isotope mass is expected.

When comparing the operational points with their respective stability boundary we find that most JET-ILLW plasmas are near the stability boundary. Only the high gas puff Γ and low δ H case is found with 30% lower $\alpha_{\max}$ which also deviates from the peeling-ballooning stability boundary. Figure 6 illustrates the ELM stability for AUG where D plasmas are close to the peeling-ballooning boundary while low δ H plasmas are to be stable against peeling-ballooning modes, in particular, with increasing gas fuelling.

It appears ELM stability cannot explain the observations in low δ H plasmas and a mechanism is required to prevent the pedestal from reaching the peeling-ballooning stability limit. High inter-ELM transport could potentially serve this function. The AUG plasma found to be most stable against peeling-ballooning modes is the one with high density fluctuations in the pedestal mentioned above. Which is an independent measurement that is consistent with the hypothesis that in AUG the inter ELM transport is important and that its properties change with isotope mass and plasma shape. Comparable measurements of the density fluctuations are not yet available for JET-ILW, still the similar phenomenology of profiles and ELM stability suggests that the same physics mechanisms

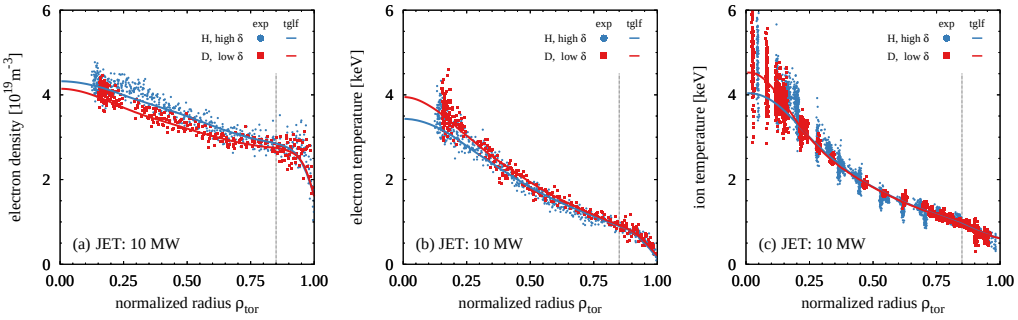

FIG. 7: Comparison of a H plasma (JPN97095) and a D plasma (JPN97036) in electron density (a), electron temperature (b) and ion temperature (c). The heating power and gas puff is matched in both cases, while the triangularity is different. The lines correspond to Astra TGLF *Sat1geo simulations with the boundary at* $\rho_{\rm tor} = 0.85$ *as indicated by the vertical black dashed line.*

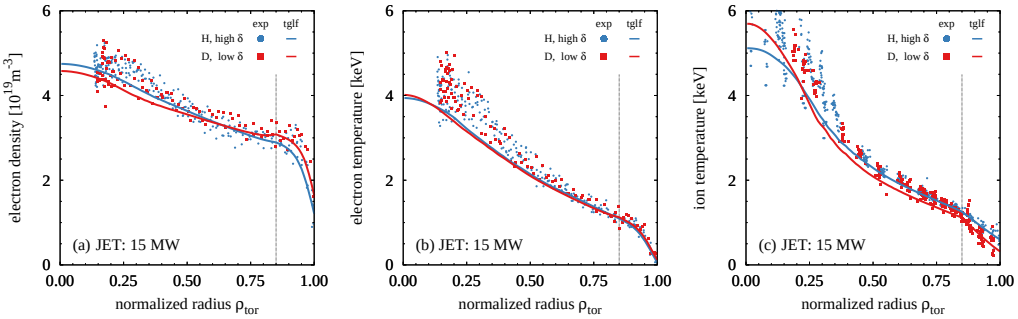

FIG. 8: Comparison of a H plasma (JPN97096) and a D plasma (JPN96831) in electron density (a), electron temperature (b) and ion temperature (c). The heating power and gas puff is matched in both cases, while the triangularity is different. The lines correspond to Astra TGLF *Sat1geo simulations with the boundary at* $\rho_{\rm tor} = 0.85$ *as indicated by the vertical black dashed line.*

dominate the plasmas in both machines.

Despite the observed differences in ELM stability, in all the plasmas ELMs are present. It is not trivial to identify the ELM type when the pedestal is deep in the peeling-ballooning stable region. The theoretical framework regarding these type of ELMs is far less developed than that for the ideal peeling-ballooning limited type-I ELMs. Although, new resistive models are being tested against experimental observations which could provide a potential explanation for this type of instability [10], the nature of these ELMs remains an open question.

3 Core transport

Very similar to the plasma edge discussed in section 2 many different factors influence the core transport. The main ion mass is expected to be one these factors. The scaling of mass and transport is also not constant and can vary depending on the plasma regime. Non-linear gyrokinetic simulations provide the foundation for our theoretical understanding. For example trapped electron mode (TEM) turbulence with a strong dependence on collisions [15] does scale differently than ion temperature gradient (ITG) driven turbulence with adiabatic electrons in the collisionless limit [4,16]. However, when considering the influence of collisions [4,12], $E \times B$ shear [17] and β stabilisation physics [17] for ITG turbulence the expected scaling with main ion mass will change. A more complete account of the different physics mechanisms depending on the main ion mass can be found in [18].

Additional to the direct impact of the main ion mass on turbulent transport, there are the indirect effects due to operational constraints which become important when testing theory against the experiment. The mass dependence in the electron-ion equipartition [19]

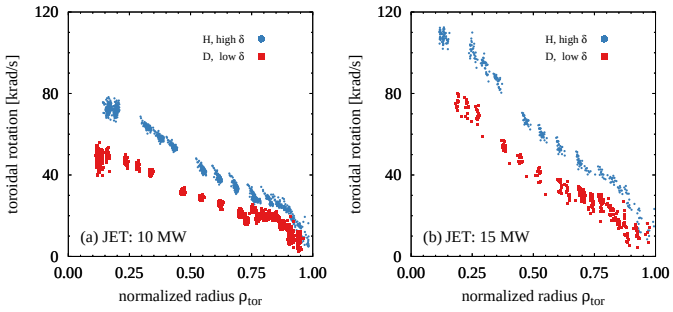

FIG. 9: Rotation profiles for the H-D comparison with matched pedestal pressure using D-NBI and different triangularity for the 10 MW cases (a) and 15 MW cases (b).

and the fast-ion slowing down [4,20] can result in different transport properties. The same is true for the mass dependence originating from the edge - discussed in section 2 - because the pedestal is strongly coupled with the plasma core [21,22]. Then there are more trivial differences like electron and ion heat fractions and different torque which need to be taken into account.

For the interpretative analysis of JET-ILW plasmas we are presenting in this section we rely on a quasilinear transport model to take into account the effects discussed above. We present simulations with ASTRA [23,24] and a recent release of TGLF [25] with the saturation rule Sat1geo [26]. We use the experimental rotation and the fast-ion density and heat flux profiles from PENCIL and PION and an experimental boundary condition at $\rho_{\mathrm{tor}} = 0.85$. The fast ions are treated as a non-resonant species in the simulations [27] and no additional effects like non-linear stabilisation of ITGs [28] are taken into account.

While TGLF with Sat1geo is one of the best models currently available for such simulations and has been steadily improved over the last years, it does not perform similarly well under all conditions [29,30]. This can influence isotope mass studies because we expect a mass dependence of the heat flux $Q \propto M^{\mu}$ with $\mu \in [-0.5, 0.5]$ while our expected temperature dependence is $Q \propto T^{2.5}$. In the data set available both mass and temperature change by a factor of two. Consequently, we are comparing an effect below 0.4 with one around 5.7 and a 10% uncertainty in the treatment of the temperature could mask any isotope effect. While the difference in the temperature is not as severe for dedicated comparison plasmas, the difference is systematic due to isotope dependence of the pedestal.

To minimize the potential uncertainties introduced by the transport model experimentally, we compare plasmas with different main ion mass and different δ, but matched pedestal conditions and matched heating and gas puffing. This is the first study of this kind in JET-ILW and allows to analyse the different contributions to the core transport with unprecedented precision.

In figure 7 the profiles for a pair of 10 MW JET-ILW discharges with moderate $\beta_{\mathrm{N}} = 1.7$ are shown and in figure 8 the same is done for profiles of discharges with 15 MW at higher $\beta_{\mathrm{N}} \geq 2.5$. Note this is the first high β H plasma which was achieved in JET. In all 4 plasmas the only auxiliary heating source is D-NBI. The solid lines in these figures are predictions from the ASTRA /TGLF simulations with the boundary at $\rho_{\mathrm{tor}} = 0.85$. For the moderate $\beta_{\mathrm{N}} = 1.7$ case shown in figure 7, TGLF predicts the profiles exceptionally well and even reproduces details like the different density peaking between H and D as well the higher core temperature peaking in the ions compared to the electrons. At higher $\beta_{\mathrm{N}} \geq 2.5$, the prediction of TGLF is not as good as with lower heating, but still reasonable since it again captures the differences in core temperature peaking between electrons and ions. Notably, the predicted profiles are practically the same for H and D, which is also the case in the experiment.

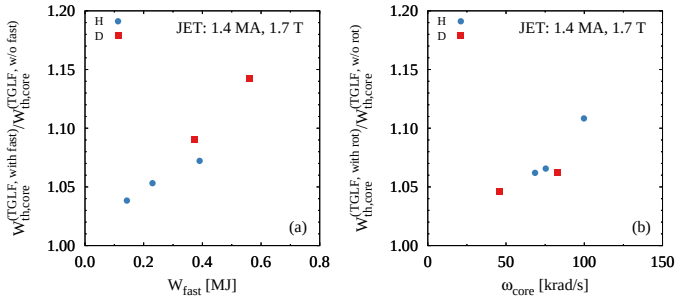

FIG. 10: Change of ASTRA TGLF *Sat1geo prediction for core contribution to thermal energy when removing fast ions (a) or setting the rotation to zero (b).*

With such a good match between theory and experiment our confidence increases that the model captures the core physics well and we can extract the different contributions to the heat transport from the simulations. This is important because despite the match in the pedestal density and temperatures there are differences between these plasmas besides the main ion mass number. Most notably are the toroidal rotation shown in figure 9 and the fast-ion content. Due to similar torque input by D-NBI, the H plasma with lower inertia rotates faster than the D plasma. While D-NBI also increases the fast-ion content compared to H-NBI, the mass dependence in the slowing down results in lower total fast-ion content in H compared to D. However, with D-NBI the difference in fast-ion content between H and D is lower than if the H plasma is heated with H-NBI.

To test the contribution of main ion mass, rotation and fast-ion content to the core transport we chose the 4 cases with matched pedestal and an additional H plasma with 10 MW of auxiliary heating with H-NBI. For these 5 plasmas two additional ASTRA /TGLF simulations were performed each - one without fast ions $n_{\mathrm{fast}} = 0$ and one without rotation $\omega = 0$.

In order to systematically compare the simulations we track the changes of the thermal core energy $W^{\mathrm{tglf}}_{\mathrm{th,core}}$ resulting from the predicted profiles. We define $W_{\mathrm{th,core}} = W_{\mathrm{th}} - W_{\mathrm{th,ped}}$ where the pedestal thermal energy $W_{\mathrm{th,ped}} = 1.5 \int p_{\mathrm{ped}}(\rho_{\mathrm{tor}}) dV$ with $p_{\mathrm{ped}}(\rho_{\mathrm{tor}}) = min\left(p_{\mathrm{ped}}(\rho_{\mathrm{tor}}), p_{\mathrm{ped}}(\rho^{\mathrm{bdry}}_{\mathrm{tor}})\right)$ and $\rho^{\mathrm{bdry}}_{\mathrm{tor}} = 0.85$ being the position of the simulation boundary.

The results of this scan are shown in figure 10 where a correlation is observed between the ASTRA /TGLF prediction and the fast-ion content W_{fast} (a) as well as the toroidal rotation in the plasma center ω_{core} (b). In the model both higher fast-ion content and higher rotation yield improved confinement, this improvement is found to be between 5-10%. These 5-10% are of the same order as the predicted impact of the isotope mass. When simulating the hydrogen discharges with deuterium mass, while keeping all other inputs - heat distribution, fast-ion content, rotation, shape and boundary condition - fixed, the cases with $M = 2$ are found to have lower core confinement by 7% for 10 MW and 12% for 15 MW. This would correspond to a weak negative mass scaling of $W_{\mathrm{th,core}} \propto M^{-0.10...-0.16}$. Not showing a gyro-Bohm scaling $M^{-0.5}$ is consistent with a code benchmark study with TGLF Sat1geo [30]. However, it is different to earlier core studies where TGLF with saturation rule Sat1 was assumed to follow gyro-Bohm [6]. This of course has a direct impact on the interpretation of the observations. In [6] the deviation between the experimental and the gyro-Bohm mass dependence was attributed to higher profile stiffness of transport in D plasmas compared to H ones. This was supported by non-linear gyrokinetic simulations [18]. In our cases with matched pedestal and a different saturation rule, the deviation between modelled and experimental profiles is much smaller and a mass dependent profile stiffness is not required to explain the observations. However, our experiment design with matched pedestal and

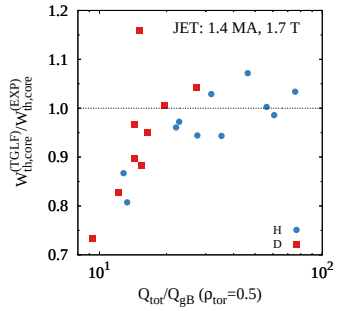

FIG. 11: Quality of the TGLF *prediction in relation to the experiment as a function of heat flux in gyroBohm units at mid-radius for the JET-ILW data set.*

matched heat sources intrinsically reduces the importance of stiffness.

When having three parameters - mass, rotation and fast-ions - change in the experiment, it is difficult to accurately determine how well each parameter change is described by the model. However, the ASTRA /TGLF predictions show similar small impact 5-10% for each parameter for these JET-ILW plasmas without any one parameter being significantly more important than the others.

Simulations were performed for the whole JET-ILW data set, including the plasmas with high δ in D and low δ in H and consequently different pedestal top pressures. This allows us to assess the quality of the TGLF predictions of the core transport. In figure 11 the deviation ratio between the experiment and the prediction is plotted as a function of the heat fluxes at mid-radius in gyroBohm units $Q_{\rm tot}/Q_{\rm gB}$. One finds that TGLF predicts the core confinement accurately within $\pm 5\%$ for $Q_{\rm tot}/Q_{\rm gB} > 15$. In particular, for H this is true despite a variation of the pedestal pressure by over a factor of 2 (cp. to figure 1).

From the points which exhibit a larger deviation between model and experiment important information can be deducted. First there is a single plasma in the data set with a 3,2 NTM. For a plasma with core MHD activity the model should overestimate the confinement, because, the magnetic island is not treated in the model. In figure 11 this plasma at $Q_{\rm tot}/Q_{\rm gB} = 15$ is clearly visible as outlier with $W_{\rm th,core}^{(\rm TGLF\ )}/W_{\rm th,core}^{(\rm EXP)} = 1.15$ as is expected. As a one point control group this increases our confidence in the validity of the remaining data set.

For $Q_{\rm tot}/Q_{\rm gB} < 15$ TGLF starts to over estimate the core transport in H and D plasmas. The two H points with $Q_{\rm tot}/Q_{\rm gB} \sim 13$ are unique, because for the first time in JET-ILW a heating power of 15 MW was introduced in a H plasma with good pedestal performance. As a thought experiment, we discuss the data set as if these two new H points were not present. Then a clear separation between H and D plasmas would remain. This might be interpreted such that theory overestimates the core heat transport in deuterium plasmas and a yet unknown isotope effect is necessary to bridge the gap between H and D plasmas. However, the separation in gyro-Bohm units is not only due to the mass dependence in the normalisation, but also due to the mass dependence in the pedestal temperature and density as described in section 2. A lower pedestal top will result in larger heat fluxes in gyro-Bohm units, despite the same experimental heat fluxes. I.e. the isotope dependence of the pedestal can have a significant impact on the interpretation of core transport modelling.

However, the new H plasmas, with high heating and high δ, show the same overestimated core heat transport in the modelling as do the D plasmas. This suggests that the shortcoming of the model for $Q_{\rm tot}/Q_{\rm gB} < 15$ does not originate in the isotope mass and is instead connected to an accurate prediction of threshold and stiffness properties of heat transport under the present conditions.

This overestimation of the core transport in H and D plasmas at low $Q_{\rm tot}/Q_{\rm gB}$ by TGLF

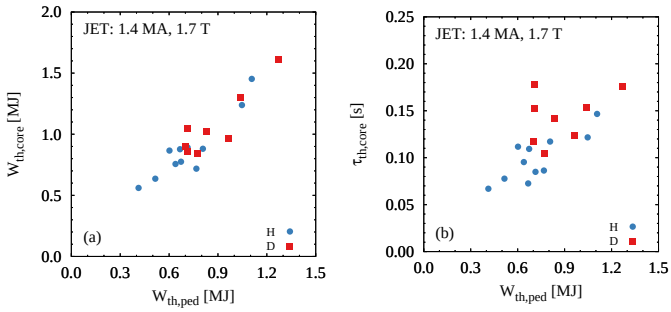

FIG. 12: Core contribution to the thermal plasma energy $W_{\mathrm{th,core}}$ (a) and thermal confinement time $\tau_{\mathrm{th,core}}$ (b) as a function of the edge contribution $W_{\mathrm{th,ped}}$ for different isotope masses in an JET-ILW power/gas scan.

was also observed in comparisons with non-linear gyrokinetic GENE simulations [30]. For such plasmas with higher β_e the nonlinear electromagnetic turbulence stabilisation - which is not present in TGLF - becomes more important [29, 31, 32]. Non-linear stabilisation of ITGs via fast ions [20, 28, 33] is likely not responsible for this difference. In the AUG core transport an empirical threshold of $W_{\mathrm{fast}}/W_{\mathrm{th}} > 1/3$ was found for NBI heated plasmas [4]. The JET-ILW 1.4 MA, 1.7 T, H and D plasmas all have $W_{\mathrm{fast}}/W_{\mathrm{th}} < 1/4$. In order to contribute to this questions nonlinear gyrokinetic simulations will be performed for our data set in the near future.

To approach this open question from the experimental side in figure 12 (a) the core-edge coupling of the plasma energy between H and D is shown. While a correlation between $W_{\mathrm{th,core}}$ and $W_{\mathrm{th,ped}}$ is not entirely surprising as it was observed before, for example, in JET-ILW [18]. In our data set the heating power is varied by over a factor of 2 and the pedestal top is varied via the shaping at constant heating power and still the correlation between edge and core holds. Further, in figure 12 (b) it is shown that the core confinement time $\tau_{\mathrm{th,core}} = W_{\mathrm{th,core}}/P_{\mathrm{sep}}$, with $P_{\mathrm{sep}} = P_{\mathrm{aux}} - P_{\mathrm{rad}}$, even increases with increasing pedestal top. This is not trivial as one would expect a strong power degradation with increasing P_{sep} which is visible in the two outliers at $W_{\mathrm{th,ped}} = 0.7$ MJ which are the D plasmas with the lowest heating power.

For our data set it is not obvious what drives this correlation. When one excludes fast ion effects a remaining candidate is β stabilisation where the experimental reasoning is that β is one of the few core parameters which is directly affected by the pedestal. However, an higher pedestal also reduces $R/L_T \propto 1/T$ and thereby the turbulence drive. Independent of the potential explanations the data shows no significant deviation between H and D plasmas. But since H plasmas are on average found with a lower pedestal energy $W_{\mathrm{th,ped}}$ than their D counterparts, also the core confinement time will be lower in H on average. Given our observations we conclude that the improvement of core confinement is not a consequence of an isotope mass dependence in the core transport, but a consequence of the core-edge coupling which is found in H and D plasmas alike.

4 Summary

While performing experiments with different main ion masses, the mass number is never the only parameter that is changing. We rather observe different overlapping effects. Most notably is the core-edge coupling. Changes in the edge will impact the core and vice versa. In the pedestal a very strong dependence on the mass number and the gas fuelling is observed. This will have direct consequences for the core confinement time - independent of the main ion mass.

Where the parameter space in AUG and JET-ILW overlaps, plasmas exhibit the same

physics responses to changes in the engineering parameters. This is found for the core transport at moderately low fast-ion content and for the strong isotope mass dependence of the pedestal, which is comparable in both machines. At the edge the inter-ELM transport is the most promising candidate to explain the experimental observations. However, the detailed underlying physics mechanisms could not be identified due to the lack of accurate transport modelling of the steep gradient region in the H-mode edge.

When the edge isotope dependence is offset by varying the triangularity at the separatrix ASTRA /TGLF (Sat1geo) simulations predict the core transport surprisingly well for moderate β. In the simulations of the core transport, fast-ion and rotation effects are found to be of the same order as the isotope mass dependence. The core transport is found near Bohm in the simulations. This is different in AUG when the fast-ion content between H and D diverges at higher NBI power density and non-linear turbulence stabilisation due to fast ions starts playing a role [4]. This is consistent with JET-ILW where the relative fast-ion content is lower than in AUG and the effect of thermal ion dilution by fast ions is sufficient to model the observations.

For the first time an isotope study between H and D could be extended to high β H plasmas. This is only possible due to the pedestal match with different δ and an increase of the heating power in H by applying D-NBI. This allows to investigate the isotope dependence of the EM stabilisation. While the experimental data suggests only a small impact of the main ion mass on the core transport also for high β plasmas, a detailed comparison to advanced theoretical models is still missing and will be subject to future investigations.

This work has been carried out within the framework of the EUROfusion Consortium and has received funding from the Euratom research and training programme 2014-2018 and 2019-2020 under grant agreement No 633053. The views and opinions expressed herein do not necessarily reflect those of the European Commission.

[1] TRANSPORT, I. P. E. G. O. C. et al., Nuclear Fusion **39** (1999) 2175.
[2] CORDEY, J., Nuclear Fusion **39** (1999) 1763.
[3] LAGGNER, F. M. et al., Physics of Plasmas **24** (2017) 56105.
[4] SCHNEIDER, P. A. et al., Nuclear Fusion **61** (2021) 036033.
[5] SCHNEIDER, P. A. et al., Plasma Physics and Controlled Fusion **63** (2021) 64006.
[6] MAGGI, C. F. et al., Plasma Physics and Controlled Fusion **60** (2018) 14045.
[7] HORVATH, L. et al., Nuclear Fusion **61** (2021) 46015.
[8] HUYSMANS, G. T. A. et al., Physics of Plasmas **8** (2001) 4292.
[9] DUNNE, M. G. et al., Plasma Physics and Controlled Fusion **59** (2017) 14017.
[10] FRASSINETTI, L., Role of the separatrix density in the pedestal performance in JET-ILW and JET-C, in *28th IAEA FEC*, Vienna, 2021.
[11] SCHNEIDER, P. A. et al., Plasma Physics and Controlled Fusion **57** (2015) 14029.
[12] BONANOMI, N. et al., Nuclear Fusion **59** (2019) 126025.
[13] BELLI, E. A. et al., Phys. Rev. Lett. **125** (2020) 15001.
[14] VIEZZER, E. et al., Nuclear Fusion **58** (2018) 26031.
[15] NAKATA, M. et al., Phys. Rev. Lett. **118** (2017) 165002.
[16] BUSTOS, A. et al., Physics of Plasmas **22** (2015) 012305.
[17] GARCIA, J. et al., Physics of Plasmas **25** (2018) 55902.
[18] WEISEN, H. et al., Journal of Plasma Physics **86** (2020) 905860501.
[19] SCHNEIDER, P. A. et al., Nuclear Fusion **57** (2017) 066003.
[20] BONANOMI, N. et al., Nuclear Fusion **59** (2019) 96030.
[21] CHALLIS, C. D. et al., Nuclear Fusion **55** (2015) 53031.
[22] GARCIA, J. et al., Nuclear Fusion **55** (2015) 53007.
[23] PEREVERZEV, G. V. et al., IPP Report **5/98** (2002).
[24] FABLE, E. et al., Plasma Physics and Controlled Fusion **55** (2013) 124028.
[25] STAEBLER, G. M. et al., Physics of Plasmas **14** (2007) 55909.
[26] STAEBLER, G. M. et al., Nuclear Fusion **57** (2017) 66046.
[27] TARDINI, G. et al., Nuclear Fusion **47** (2007) 280.
[28] CITRIN, J. et al., Phys. Rev. Lett. **111** (2013) 155001.
[29] REISNER, M. et al., Nuclear Fusion **60** (2020) 82005.
[30] MARIANI, A. et al., Nuclear Fusion **61** (2021) 66032.
[31] CITRIN, J. et al., Nuclear Fusion **54** (2014) 23008.
[32] DOERK, H. et al., Plasma Physics and Controlled Fusion **58** (2016) 115005.
[33] Di Siena, A. et al., Physics of Plasmas **25** (2018) 42304.